tvst

DOI: 10.1167/tvst.1.3.2

Article

The Oral Iron Chelator Deferiprone Protects Against Retinal Degeneration Induced through Diverse Mechanisms

Majda Hadziahmetovic[1], Miroslav Pajic[2], Steven Grieco[1], Ying Song[1], Delu Song[1], Yafeng Li[1], Alyssa Cwanger[1], Jared Iacovelli[1], Sally Chu[1], Gui-shuang Ying[3], John Connelly[4], Michael Spino[4], and Joshua L. Dunaief[1] ✉

[1] F.M. Kirby Center for Molecular Ophthalmology, Scheie Eye Institute, University of Pennsylvania, Philadelphia, PA
[2] Department of Electrical and Systems Engineering, University of Pennsylvania, Philadelphia, PA
[3] Center of Preventive Ophthalmology and Biostatistics, Scheie Eye Institute, University of Pennsylvania, Philadelphia, PA
[4] ApoPharma, Inc., Toronto, Ontario, Canada

Correspondence: Joshua L. Dunaief, 305 Stellar Chance Labs, 422 Curie Boulevard, Philadelphia, PA 19104, USA. e-mail: jdunaief@upenn.edu

Received: 4 May 2012
Accepted: 20 August 2012
Published: 25 October 2012

Keywords: retinal degeneration; deferiprone; iron

Citation: Hadziahmetovic M, Pajic M, Grieco S. The oral iron chelator deferiprone protects against retinal degeneration induced through diverse mechanisms. Tran Vis Sci Tech. 2012;1(3):2, http://tvstjournal.org/doi/full/10.1167/tvst.1.3.2, doi:10.1167/tvst.1.3.2

Purpose: To investigate the effect of the iron chelator deferiprone (DFP) on sodium iodate ($NaIO_3$)–induced retinal degeneration and on the hereditary retinal degeneration caused by the *rd6* mutation.

Methods: Retinas from $NaIO_3$-treated C57BL/6J mice, with or without DFP cotreatment, were analyzed by histology, immunofluorescence, and quantitative PCR to investigate the effect of DFP on retinal degeneration. To facilitate photoreceptor quantification, we developed a new function of MATLAB to perform this task in a semiautomated fashion. Additionally, *rd6* mice treated with or without DFP were analyzed by histology to assess possible protection.

Results: In $NaIO_3$-treated mice, DFP protected against retinal degeneration and significantly decreased expression of the oxidative stress–related gene heme oxygenase-1 and the complement gene *C3*. DFP treatment partially protected against $NaIO_3$-induced reduction in the levels of mRNAs encoded by visual cycle genes rhodopsin (*Rho*) and retinal pigment epithelium–specific 65 kDa protein (*Rpe65*), consistent with the morphological data indicating preservation of photoreceptors and RPE, respectively. DFP treatment also protected photoreceptors in *rd6* mice.

Conclusions: The oral iron chelator DFP provides significant protection against retinal degeneration induced through different modalities. This suggests that iron chelation could be useful as a treatment for retinal degeneration even when the main etiology does not appear to be iron dysregulation.

Translational Relevance: These data provide proof of principle that the oral iron chelator DFP can protect the retina against diverse insults. Further testing of DFP in additional animal retinal degeneration models at a range of doses is warranted.

Introduction

The retinal pigment epithelium (RPE) plays a key role in photoreceptor support. It participates in phagocytosis of the shed outer segments of photoreceptors, directional transport of nutrients, and removal of waste products, as well as visual pigment transport and regeneration.[1,2] RPE damage can result in photoreceptor degeneration, visual impairment, and irreversible blindness.[3] Decreases in RPE density and pigment, together with lipofuscin accumulation, are part of physiological aging.[4] There is a spectrum of retinal disorders of environmental or genetic etiology in which the primary site of pathogenesis is either RPE or adjacent photoreceptors. Oxidative stress has been implicated in a variety of eye diseases, including age-related macular degeneration, glaucoma, and retinitis pigmentosa.

RPE cells and photoreceptors are particularly susceptible to oxidative stress due to high oxygen tension, large numbers of mitochondria, and abundant polyunsaturated fatty acids in photoreceptor membranes.[5] Age-related macular degeneration (AMD) is

the most common cause of irreversible vision loss in the elderly in the Western world. Although the pathogenesis of AMD is not fully understood, in addition to inflammation, complement activation, and other hereditary and environmental factors,[6–8] oxidative stress is important.[9,10] Epidemiologic studies showing that dietary antioxidants reduce the risk of developing advanced AMD support this assertion.[11] Morphologic changes in AMD include lipofuscin accumulation and drusen formation, as well as subsequent RPE and photoreceptor cell loss, sometimes associated with neovascularization.[12]

In our previous work we have shown higher iron levels in AMD retinas than in age-matched controls,[13] suggesting that iron-mediated oxidative stress may contribute to retinal degeneration in AMD. Mice deficient in the ferroxidases ceruloplasmin and hephaestin accumulate iron in the retina and subsequently have retinal degeneration with features of AMD.[14,15] In these mice we found that iron chelation with the orally absorbed and cell-permeant iron chelator deferiprone (DFP) ameliorated oxidative stress and protected against iron overload–induced retinal degeneration.[16] Therefore, cell-permeant iron chelators may serve as protective agents against human retinal disorders in which iron accumulation is a main culprit.

The goal of the present study was to test whether iron chelation might protect not only against iron overload–induced retinal degeneration, in the presence of excess iron, but also against retinal degeneration initiated by other mechanisms. Prior studies have shown that the iron chelator deferoxamine can protect against retinal light damage[17] and retinal ischemia reperfusion injury.[18] However, deferoxamine is not a viable candidate as a therapy for retinal diseases since it is associated with retinal toxicity.[19] We chose to test the drug DFP, recently approved by the Food and Drug Administration, because it is orally absorbed and has not been associated with retinal toxicity in patients or mice.[16] In this study we tested DFP's ability to prevent $NaIO_3$-induced retinal degeneration. $NaIO_3$ is a retinotoxin, and its systemic administration selectively damages RPE and photoreceptors. Additionally we tested the effect of DFP on a mouse model with hereditary retinal degeneration due to *rd6* mutation. The *rd6* mutation affects the *Mfrp* gene, a frizzled-related gene expressed in the RPE.[20] Mice with this mutation have a slowly progressive loss of photoreceptors over many months.[21] Our results suggest that iron chelation may serve as a protective agent not only against iron overload–induced retinal degeneration, but also against retinal disorders in which iron dysregulation is not the primary cause.

Materials and Methods

Animals

Female C57BL/6J wild type (WT) mice, 10 weeks of age, and female B6.C3Ga-*Mfrp*^{rd6}/J mice, 4 weeks of age, were obtained from The Jackson Laboratory (Bar Harbor, ME). The animals were fed ad libitum and maintained on a 12 hour/12 hour light/dark cycle. All procedures were approved by the Institutional Animal Care and Use Committee of the University of Pennsylvania and complied with the ARVO Statement for the Use of Animals in Ophthalmic and Vision Research.

Deferiprone Treatment

C57BL/6J mice were divided into three groups ($n=4$ each). One group (control) was untreated; one group was treated with sodium iodate ($NaIO_3$) only; and the third group was treated with 1 mg/mL DFP (Apo-Pharma, Inc., Toronto, Ontario, Canada) in drinking water for 21 days (14 days before and 7 days after a single injection of $NaIO_3$). Additionally, DFP-treated mice were gavaged with 75 mg/kg DFP in 0.5% carboxymethylcellulose sodium salt (Sigma-Aldrich, St. Louis, MO) once per day for 14 days (7 days before and 7 days after the sodium iodate injection). B6.C3Ga-*Mfrp*^{rd6}/J mice were divided into two groups ($n = 4$ each); one group was treated with 1 mg/mL DFP in drinking water for 5 months beginning at 4 weeks of age, and the control group received no DFP.

$NaIO_3$ Treatment

Sodium iodate ($NaIO_3$; Sigma-Aldrich) was dissolved in physiological saline at a concentration of 1%. Fourteen days after start of treatment with 1 mg/mL DFP and 7 days after initiation of gavage with 75 mg/kg DFP, $NaIO_3$ solution was injected via the tail vein at a dose of 25 mg/kg. The DFP-untreated group was injected in the same manner. The mice were returned to the animal facility for an additional 7 days. No changes in body weight were observed following either $NaIO_3$ or DFP treatment.

Morphologic Analysis

After fixation in 2% paraformaldehyde and 2% glutaraldehyde, the cornea and lens were removed, leaving an "eye cup" consisting of retina/choroid/

sclera. The eye cups were then dehydrated in increasing concentrations of ethanol, infiltrated overnight, and embedded the next day in plastic (JB4 Solution A; Polysciences, Inc., Warrington, PA). For standard histology, 3 μm thick plastic sections were toluidine blue stained by incubation of the sections in 1% toluidine blue O and 1% sodium tetraborate decahydrate (Sigma-Aldrich) for 5 seconds. Stained sections were observed and photographed with a TE300 microscope (Nikon, Tokyo, Japan). Biological and technical triplicates were counted for DFP-treated and untreated B6.C3Ga-*Mfrp*^{rd6}/J mice, while biological triplicates were used for $NaIO_3$-treated and $NaIO_3$- and DFP-cotreated C57BL/6J mice.

MATLAB Function for Photoreceptor Nuclei Count

Due to the palisading degeneration of the outer nuclear layer (ONL) following $NaIO_3$ injection, we were unable to use ONL thickness measurements as an indicator of photoreceptor number. Therefore, we created a MATLAB function to facilitate comparison between the number of photoreceptor nuclei in $NaIO_3$-treated and $NaIO_3$- and DFP-cotreated mice. The procedure was used to automatically count the number of photoreceptor nuclei in each retina by processing the images obtained from our experiments. MATLAB, a widely used numerical computing environment and a programming language, was developed by Mathworks, Inc. (Natick, MA) and contains libraries (i.e., toolboxes) that provide software support for signal and image processing.

The color image of a selected segment of the ONL was converted to a grayscale image, and a MATLAB built-in function was utilized to extract the part of the image within the contour, thus extracting the image of the region of interest. Contrast-limited adaptive histogram equalization was performed to enhance the contrast of images (emphasize differences between white and nonwhite areas) and highlight the cell edges in the grayscale image. To enable separating photoreceptor nuclei from the rest of the background, the procedure converted the images into black-and-white images by designating all pixels above a threshold as white. In grayscale images, the color of each pixel was described as a number that represents a level of gray between 0 and 255 (0 corresponds to black and 255 to white). On the other hand, black-and-white images used only two color levels to describe the color of each pixel—white or black. The black-and-white (i.e., binary) picture was then filtered to remove "noise" pixels—all connected components on the image that had fewer than the specified number of pixels. Finally, in the picture obtained, the procedure determined the number of nuclei. Note that our procedure was unlike image processing established for blood cell counts[22]; we did not map each component into a single cell in the initial image. Due to the overlapping nuclei it was possible for two (or more) nuclei from the initial image to result in a single connected component in the final image. To derive the final count of nuclei, we assigned each connected component to the appropriate number of nuclei by accounting for the area of the image covered by the component. In this case, the number of nuclei extracted from a component was equal to the lowest integer that was less than the ratio between the component's area and a predefined nucleus-area threshold.

The main difficulty with the aforementioned procedure was determining the threshold level to be used to convert the grayscale images to black-and-white images, along with the threshold area size used to extract the final count. To derive the threshold level for the image conversion, the procedure used a scaled output of the MATLAB graythresh function. The scaling factor was obtained using a configuration procedure that required the user's input. In the initial image, the user highlighted a small subsection in which the number of cells was manually counted. During the calibration, scaling parameters were selected that minimized the error between the automatically computed number of cells and the number of cells provided by the user. Note that during calibration the cell size parameter was obtained as the size of the largest cell that had been properly extracted. For an illustration of the calibration procedure, consider the images in Figure 1C.

Flat-mount Immunofluorescence

For whole-mount retina staining, the globes were fixed in 4% paraformaldehyde for 10 minutes, and the eye cups were generated by removing the anterior segment. The neurosensory retina was also removed. The eye cups were then blocked in buffer containing 5% normal donkey serum (Jackson ImmunoResearch Laboratories, Inc., West Grove, PA) and 0.3% Triton X-100 (Sigma-Aldrich) for 1 hour at room temperature, followed by incubation with primary antibody overnight at 4°C. The primary antibody was rabbit anti-ZO-1 at 1:100 dilution (Invitrogen Corporation, Carlsbad, CA), and it was detected using fluorophore-labeled secondary antibodies (Jackson ImmunoResearch Laboratories, Inc.). The eye cups were then flattened on a glass slide with four relaxing incisions. The flat mounts were mounted using medium for fluorescent microscopy (KPL, Gaithersburg, MD).

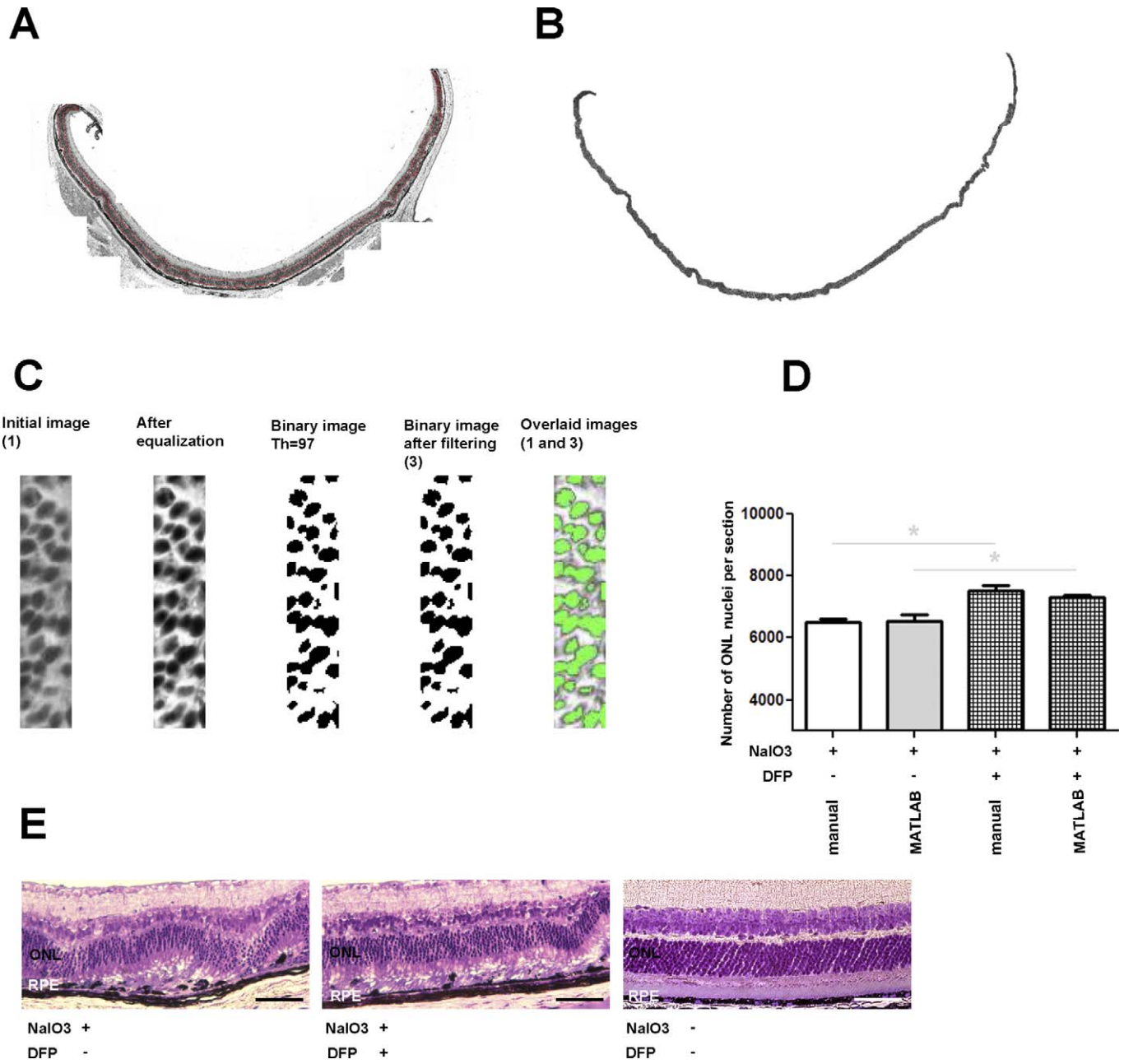

Figure 1. Bright-field photomicrographs of plastic sections (A, B, C) illustrate photoreceptor nuclei selection by MATLAB to count the number of nuclei within the ONL. Bar graph (D) shows number of ONL nuclei in retinas from mice treated with $NaIO_3$ only, or with $NaIO_3$- and DFP-cotreated retinas calculated manually (first and third) or calculated by MATLAB function (second and fourth). Manual or MATLAB counting indicated a significantly higher number of nuclei within ONL in DFP-cotreated than in $NaIO_3$ only–treated samples. The MATLAB function deviated from manual counting by approximately 6% for $NaIO_3$ and 4% for DFP- and $NaIO_3$-cotreated samples. Bright-field photomicrographs (E; $NaIO_3$ only–treated retina, left; $NaIO_3$ and DFP cotreated, center; untreated, right) show that DFP treatment ameliorated $NaIO_3$-induced retinal degeneration. Scale bar 50 μm. ONL, outer nuclear layer; RPE, retinal pigment epithelium.

Fluorescence microscopy was performed with identical exposure parameters within the same area of peripheral retina (model TE300 microscope [Nikon]). The number of RPE cells was counted using NIS-Elements BR 3.1 (Nikon) software within the corresponding areas.

Neurosensory Retina and RPE Isolation

Purified RPE cells were isolated by removing the anterior segment (cornea, iris, and lens) from enucleated mouse eyes after a two-step digestion. Briefly, whole eyes were incubated at 37°C for 40

minutes in 2% w/v dispase in 1× Hanks' balanced salt solution with Ca^{2+} and Mg^{2+} (HBSS+) (Invitrogen Corporation). Following digestion with dispase, slits were made in the cornea with a scalpel blade, and the eyes were incubated for an additional 10 minutes in 1 mg/mL hyaluronidase in Hanks' balanced salt solution without Ca^{2+} and Mg^{2+} (HBSS–). Following two washes in HBSS+, the anterior segment was removed and the eye cup was placed in HBSS–, where the neurosensory retina was removed. The neurosensory retina was frozen on dry ice and stored at −80°C until the RNA isolation was performed with the RNeasy Mini Kit (Qiagen Inc., Valencia, CA) according to the manufacturer's protocol. The RPE cells were gently brushed from the eye cup in fresh HBSS–, collected, and pelleted at 1200*g* for 15 minutes. The supernatant was removed, and the cells were stored at −80°C until the RNA isolation was performed with the RNeasy Micro Kit (Qiagen Inc.) according to the manufacturer's protocol.

Quantitative Real-time PCR

Neurosensory retina and RPE samples were analyzed using quantitative RT-PCR (qPCR) for gene expression. The RNA was quantified with a spectrophotometer (Nanodrop Technologies, Wilmington, DE) and stored at −80°C. cDNA was synthesized using TaqMan Reverse Transcription Reagents (Applied Biosystems, Inc., Carlsbad, CA), according to the manufacturer's protocol. TaqMan gene expression assays were obtained from Applied Biosystems and used for PCR analysis. Probes used were transferrin receptor (*Tfrc*, Mm00441941_m1), heme oxygenase-1 (*Hmox1*, Mm00516005_m1), rhodopsin (*Rho*, Mm00520345_m1), complement component 3 (*C3*, Mm00437858_m1), and retinal pigment epithelium 65 (*Rpe65*, Mm00504133_m1). Eukaryotic 18S rRNA (Hs99999901_s1) served as an internal control. Real-time TaqMan RT-PCR (Applied Biosystems, Inc.) was performed on an ABI Prism 7500 Sequence Detection System (Applied Biosystems, Foster City, CA) using the $\Delta\Delta C_T$ method, which provides normalized expression values. The amount of target mRNA was compared among the groups of interest. All reactions were performed in biological (three mice) and technical (three qPCR replicates per mouse) triplicates.

Statistical Analysis

For cell counts and gene expression data, the mean and standard error of the mean (SEM) were calculated for each group. The two-group *t*-test was used to compare the means between two groups, and one-way analysis of variance (ANOVA) was used to compare the means among three groups, followed by Tukey's post hoc test for pairwise comparisons. These statistical analyses were performed with GraphPad software (GraphPad Prism 5; GraphPad Software, Inc., San Diego, CA). For the counts of photoreceptor nuclei in B6.C3Ga-*Mfrp*^{rd6}/J mice, mean and standard error were calculated at each distance from the optic nerve head. A generalized linear model that accounts for the correlation among nuclei counts across various distances in three different sections from each eye was used to compare the overall differences in photoreceptor nuclei counts between two groups (DFP treated vs. untreated), followed by the test of their difference at each distance level if overall difference was significantly different. Generalized models were executed using PROC GENMOD in SAS 9.2 (SAS Inc., Cary, NC). A P value <0.05 was considered to be statistically significant. All results are presented as means ± SEM.

Results

Deferiprone Protects Photoreceptor Nuclei against $NaIO_3$ Toxicity

To investigate the effect of DFP on $NaIO_3$-induced photoreceptor death, we created a MATLAB function to count remaining photoreceptors. In DFP-cotreated animals, the number of photoreceptor nuclei was significantly higher than that in the animals given $NaIO_3$ alone when counted both manually and by the MATLAB function (Fig. 1D). The number of remaining photoreceptors was 13.7% greater in the DFP-treated mice. Additionally, DFP treatment ameliorated $NaIO_3$-induced retinal degeneration (Fig. 1E). DFP-cotreated eyes had a thicker ONL and better-preserved photoreceptor inner and outer segments (Fig. 1E, center panel) than eyes treated with $NaIO_3$ alone (Fig. 1E, left panel). RPE disorganization and thinning were also less severe following $NaIO_3$ treatment if the mice were cotreated with DFP (quantified below).

Deferiprone Treatment Ameliorates the Toxic Effect of $NaIO_3$ on RPE Cells

As assessed by tight-junction protein (ZO-1) immunofluorescence (Fig. 2A), flat mounts of the peripheral retina showed RPE cells with normal morphology and minimal autofluorescence in $NaIO_3$/DFP-treated mice (middle row). The same region in samples from mice treated only with $NaIO_3$

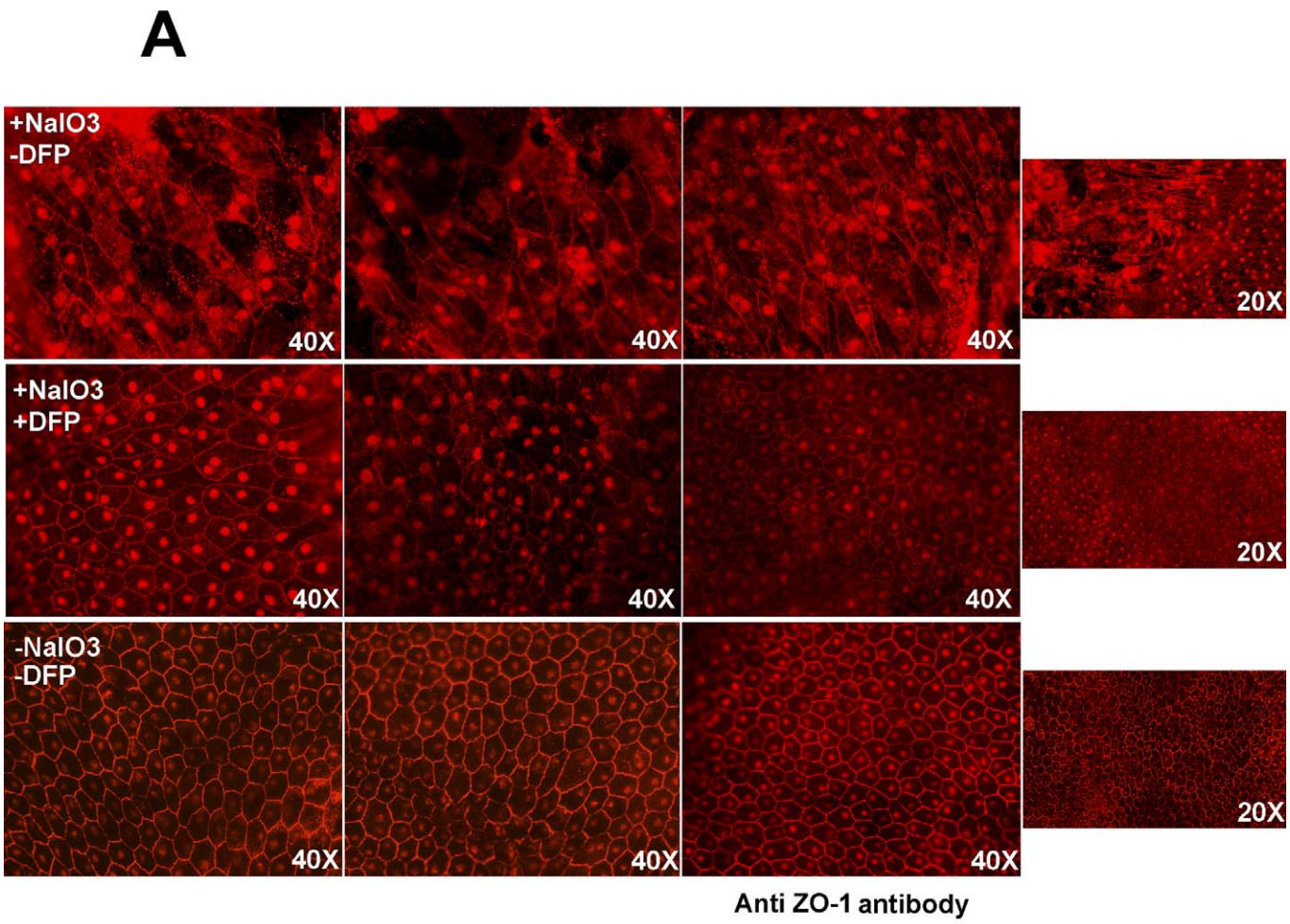
A
+NaIO3
-DFP
40X
40X
40X
20X
+NaIO3
+DFP
40X
40X
40X
20X
-NaIO3
-DFP
40X
40X
40X
20X
Anti ZO-1 antibody

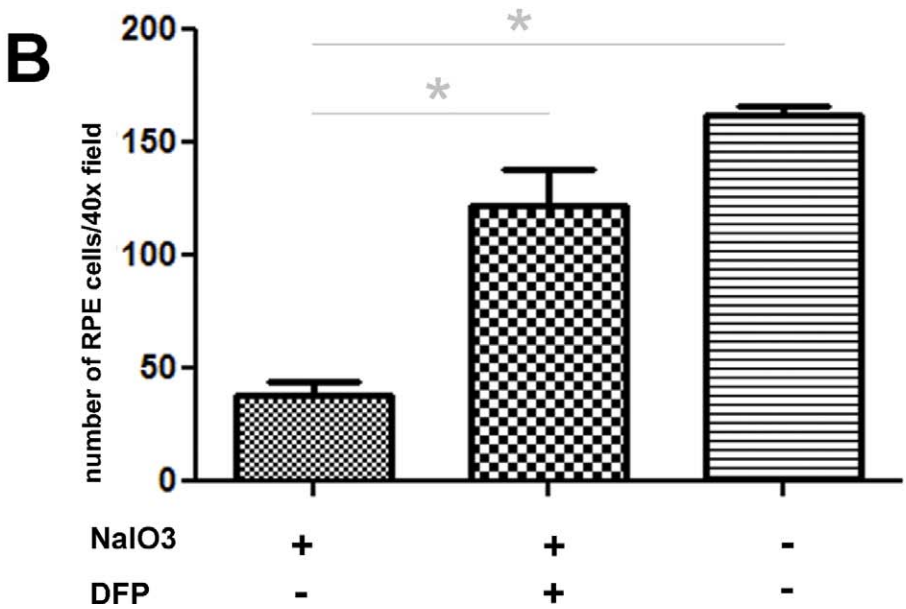
B
200
150
100
50
0
number of RPE cells/40x field
*
*
NaIO3
DFP
+
-
+
+
-
-

(top row) exhibited massively hypertrophic and irregular RPE cells, with accumulation of autofluorescent material. Autofluorescence has been used as a measure of the extent of the RPE damage after injection of $NaIO_3$.[23] Mice treated with $NaIO_3$ alone had 25.0% of the normal number of cells, and mice treated with DFP plus $NaIO_3$ had 90.7% of the normal number (Fig. 2B).

Gene Expression Changes following $NaIO_3$ and Deferiprone Treatment

To investigate the effect of DFP on gene expression within the neurosensory retina (NSR) and isolated RPE cells, qPCR with transferrin receptor (*Tfr*), rhodopsin (*Rho*), retinal pigment epithelium 65 (*Rpe65*), heme oxygenase-1(*Hmox1*), and complement component 3 (*C3*) probes was performed following $NaIO_3$ treatment. Within the NSR, DFP treatment caused a significant increase in *Tfr* mRNA (Fig. 3A), as expected, since diminished labile iron levels cause accumulation of the *Tfr* mRNA.[16] Additionally in the same samples, DFP treatment partially protected against the $NaIO_3$-mediated reduction in *Rho* mRNA levels (Fig. 3B). Relative to the $NaIO_3$ only–treated group, levels in DFP-treated mice were 41.3% higher. Levels of mRNAs associated with retinal stress and degeneration, *Hmox1* and *C3*, increased significantly within the NSR following treatment with $NaIO_3$, but this increase was significantly diminished by coadministration of DFP (Figs. 3C, 3D). Results obtained from isolated RPE cells, similarly to those obtained from NSR, suggested a protective effect of DFP on $NaIO_3$-induced retinal damage. Consistent with our prior results,[16] DFP treatment did not increase *Tfr* expression within the RPE (Fig. 4A), but it significantly ameliorated the reduction of *Rpe65* mRNA levels induced by $NaIO_3$ (80% higher with DFP treatment, Fig. 4B). Similar to the NSR results, mRNA levels of *Hmox1* and *C3* were significantly upregulated following the treatment with $NaIO_3$, and markedly less so in mice cotreated with DFP (Figs. 4C, 4D). All gene expression results were compared with those from control mice treated with neither DFP nor $NaIO_3$.

Deferiprone Protects rd6 Mice from Retinal Degeneration

Homozygous *rd6* mice exhibit an early onset and slow retinal degeneration.[21] In these mice, alterations in the photoreceptor layer can be seen shortly after the retina develops. Photoreceptor cells degenerate from the normal 10- to 12-cell-layer thickness to 4 to 6 cell layers by 6 months of age. Morphologic analysis was done at age 6 months following 5 months of treatment with DFP, and the numbers of photoreceptor nuclei in each eye were counted in three different sagittal sections through the optic nerve head. DFP conferred significant morphologic preservation of photoreceptors throughout the retina (Fig. 5A). Untreated eyes (Fig. 5B) had more severe thinning of the photoreceptor nuclear layer than those from mice treated with DFP; preservation of the ONL was evident in the latter (Fig. 5B, overall comparison for the entire retina $P < 0.0001$).

Discussion

In this study we investigated whether systemic administration of the iron chelator DFP effectively prevents retinal degeneration induced by modalities other than iron overload. Our data showed that in C57BL/6J mice, DFP diminished $NaIO_3$-induced upregulation of antioxidant and complement genes and protected against the ONL thinning caused by $NaIO_3$. DFP protected against $NaIO_3$-induced reduction in the levels of visual cycle genes *Rho* and *Rpe65*, consistent with retinal protection. Also, DFP treatment ameliorated hereditary retinal degeneration due to the *rd6* mutation in B6.C3Ga-*Mfrp*^{rd6}/J mutant mice.

Iron chelation is a widely used treatment for acute iron toxicity and chronic transfusional iron overload. Recently, iron chelation has been tested in patients with neurodegenerative disorders who have only localized brain iron dysregulation. Three widely used iron chelators are deferoxamine, deferasirox, and DFP. As previously mentioned, deferoxamine has proved to be protective against retinal light damage[17] and ischemia reperfusion injury.[18] Additionally, it has been demonstrated that treatment with deferoxamine

←

Figure 2. Flat mounts of the RPE/choroid/sclera immunolabeled with ZO-1 for mice treated with $NaIO_3$, mice treated with $NaIO_3$ plus NaIO3, and untreated control (A). Each row contains images from three mice. Mice treated with $NaIO_3$ but not treated with DFP had hypertrophic, irregular, and autofluorescent RPE cells (upper row). RPE cells from mice treated with $NaIO_3$ and DFP (middle row) appear more similar to untreated controls (bottom row). Graph showing number of RPE cells per designated field (B). The asterisk denotes significant difference ($P < 0.05$) between the means of the groups.

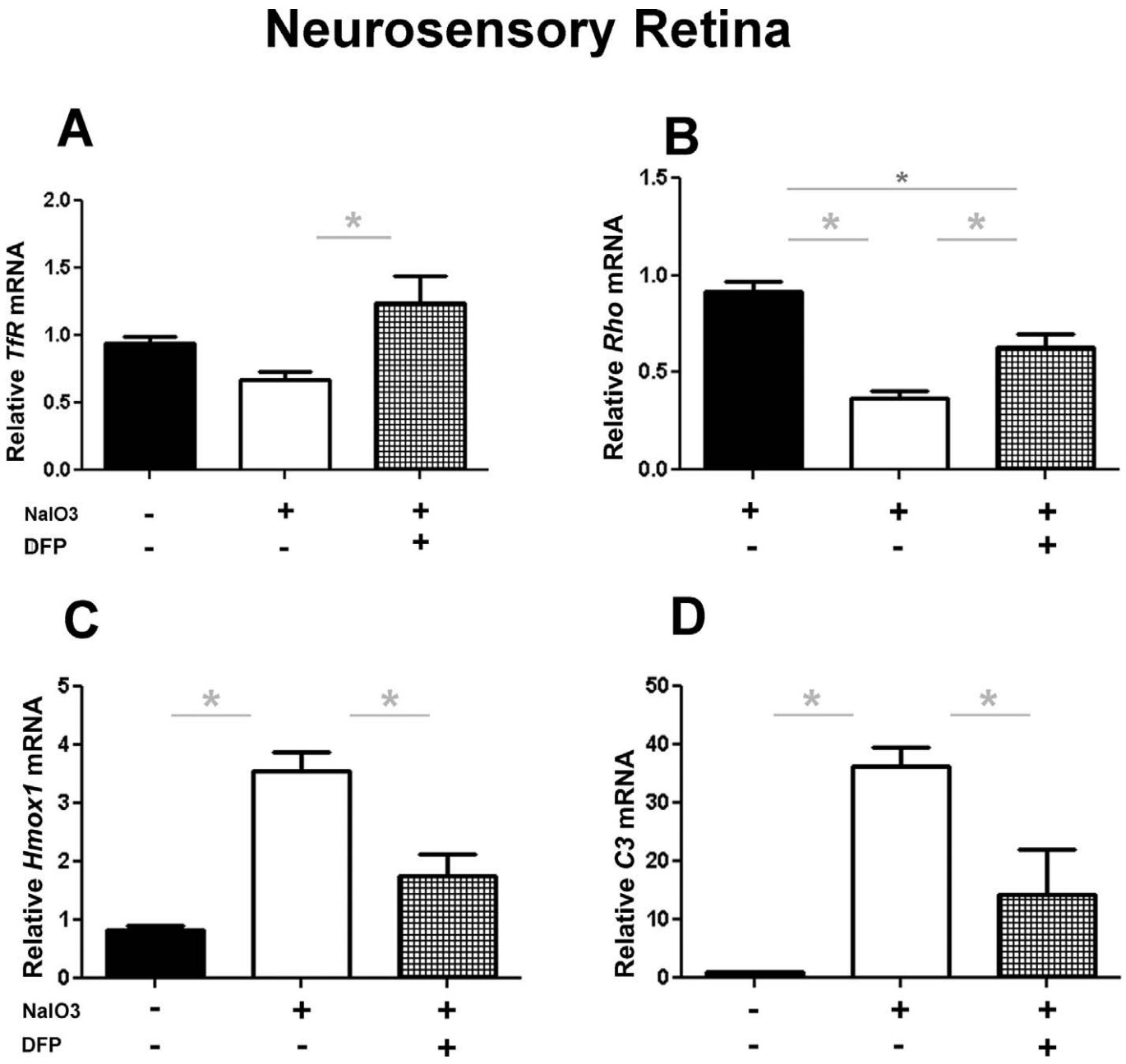

Figure 3. Graphs showing qPCR results illustrate the effect of DFP on $NaIO_3$-induced changes in gene expression within the neurosensory retina. DFP treatment significantly increased *Tfr* mRNA levels relative to the control group (DFP and $NaIO_3$ untreated) and the $NaIO_3$ only–treated group (A). *Rho* mRNA levels (B) were significantly higher in the DFP-treated group. DFP treatment significantly decreased *Hmox1* and *C3* mRNA (C, D) following $NaIO_3$ administration. ANOVA with a Tukey post hoc test was used to compare the means between the groups. The asterisk denotes significant difference ($P < 0.05$) between the means of the groups.

provides both functional and structural rescue in the *rd10* mouse model of retinitis pigmentosa.[24] However, the clinical use of deferoxamine is associated with retinal toxicity. With regard to deferasirox, the absence of evidence that it can decrease brain or retinal iron levels significantly limits its use as a treatment for neurodegenerative disorders. DFP is an orally absorbed, low molecular weight iron chelator that easily penetrates cells. DFP can cross the blood–brain barrier and decrease brain iron levels in patients with Friedreich's ataxia, with improved motor function in some patients.[25] We have shown previously that orally administered DFP can cross the blood–retinal barrier, and protect against retinal degenera-

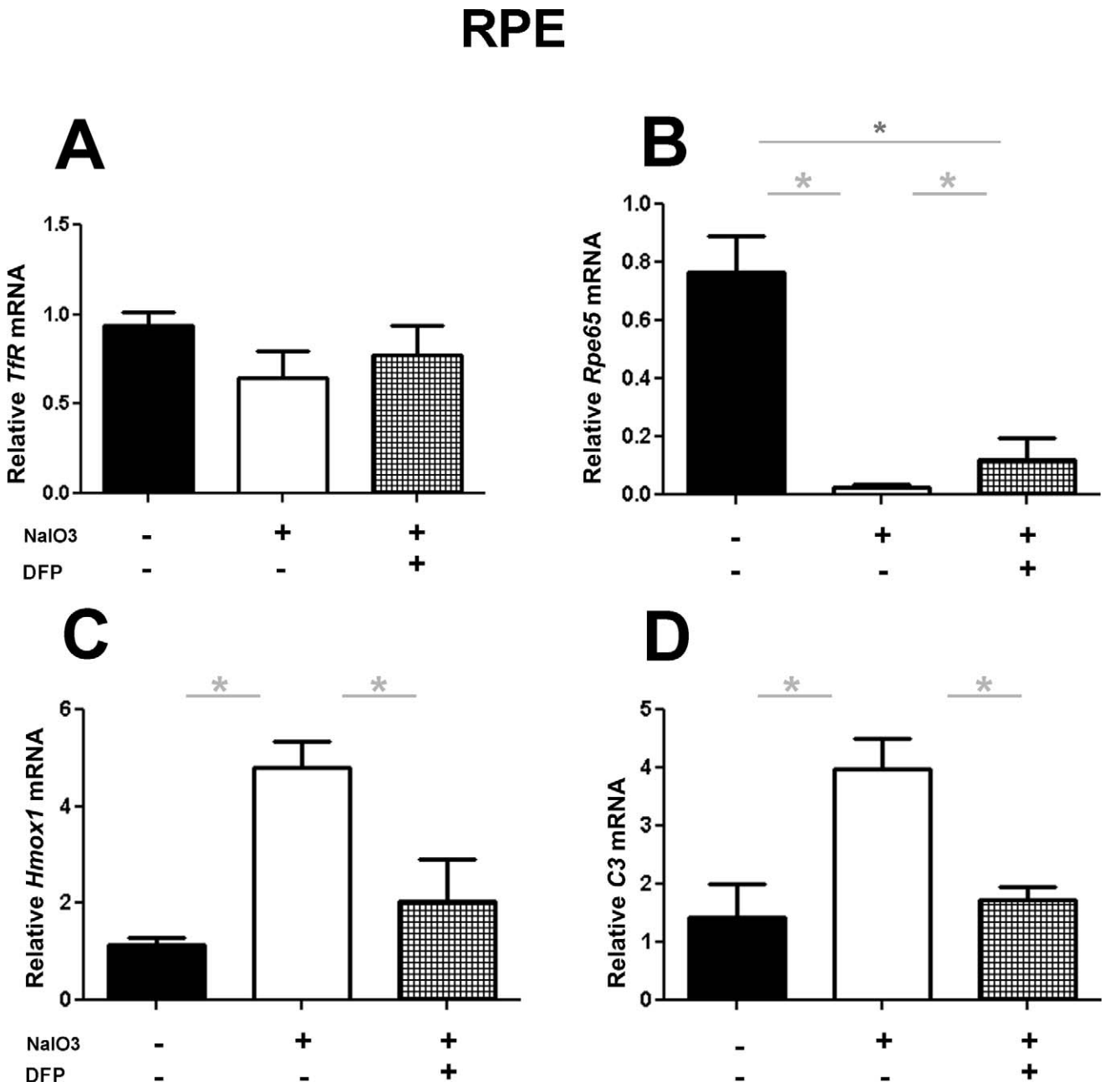

Figure 4. Effect of DFP on $NaIO_3$-induced changes in gene expression within the RPE shown by qPCR. DFP treatment caused no changes in *Tfr* mRNA levels relative to the control group (DFP and $NaIO_3$ untreated) and the $NaIO_3$ only–treated group (A). *Rpe65* mRNA levels were significantly higher in the DFP-treated group (B). DFP treatment significantly decreased *Hmox1* and *C3* mRNA (C, D) following $NaIO_3$ tail veil injection. ANOVA with a Tukey post test was used to compare the means between the groups. The asterisk denotes significant difference ($P < 0.05$) between the means of the groups.

tion associated with a local excess of iron in ceruloplasmin/hephaestin knockout mice. Recently, we have found that DFP can protect photoreceptors against light-induced damage in which iron dysregulation is not the proximal cause of the degeneration.[26]

In this study, to confirm that DFP can cross the blood–retinal barrier and decrease labile iron pools, we examined *Tfr* mRNA levels following DFP treatment. *Tfr* stability is regulated by labile iron levels, with decreased labile iron resulting in increased *Tfr* mRNA.[27] Within the NSR, DFP treatment increased *Tfr* mRNA (Fig. 3A), indicating that in addition to crossing the blood–retinal barrier, it decreases the labile iron pool. The observed change in *Tfr* mRNA in

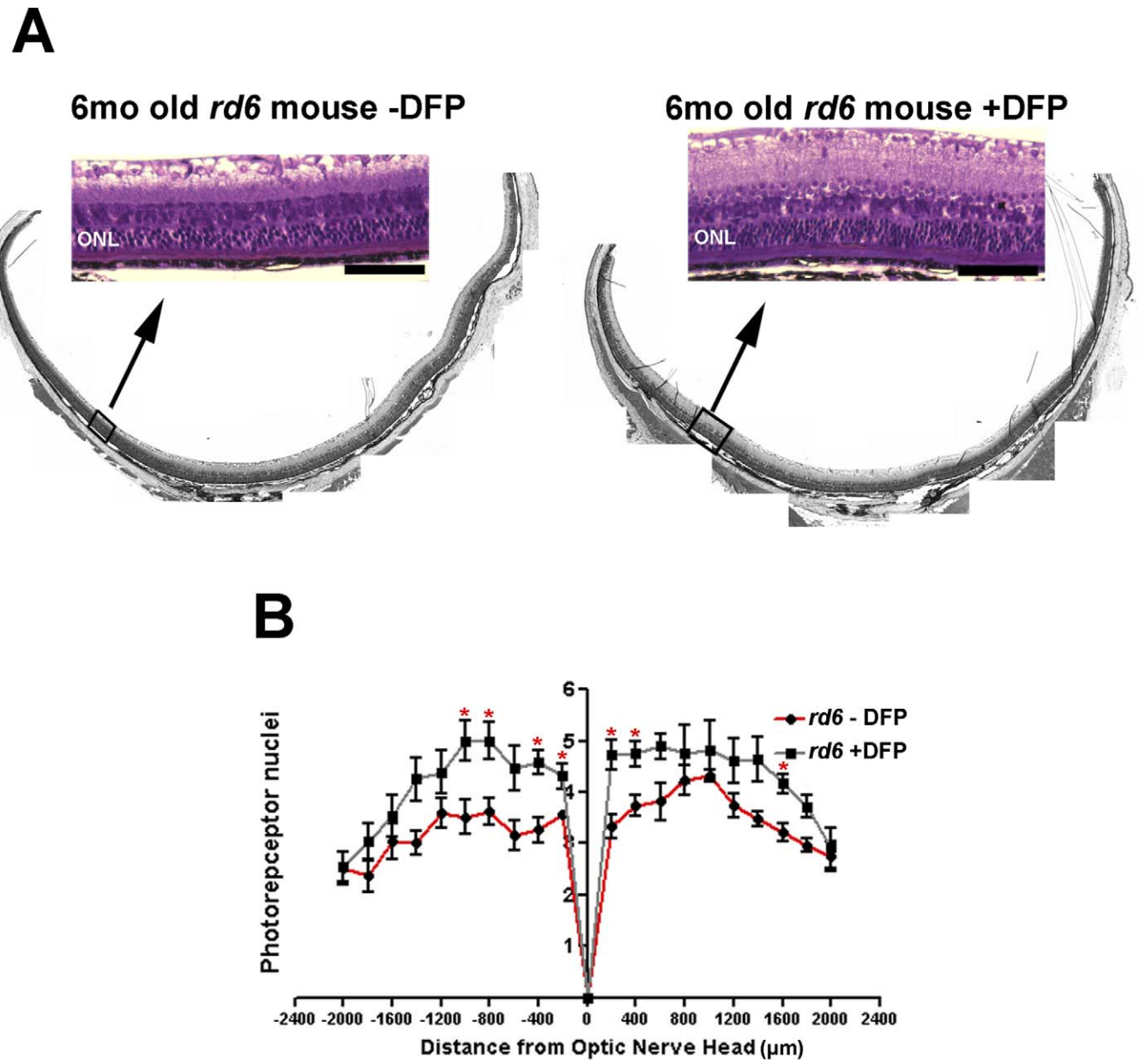

Figure 5. Bright-field micrographs of plastic sections show that compared with DFP-untreated *rd6* mice (A, left), DFP-treated mice (A, right) had better preservation of photoreceptor morphology with thicker ONL and inner and outer segments. Scale bar 50 μm. ONL, outer nuclear layer. Thickness of the ONL of DFP-untreated (red) and DFP-treated (gray) *rd6* mice at 6 months of age is shown in a spider diagram (B). The measurements were taken at 400 μm intervals from the optic nerve head (ONH). The asterisk denotes significant difference ($P < 0.05$) between the means of two groups.

the neural retina, as well as no change within the RPE (Fig. 4A), was consistent with our previously published data. Thus, DFP may protect the RPE in the $NaIO_3$ model by chelating enough labile iron in the RPE to be protective (but not enough to change *Tfr* mRNA levels), or through iron chelation in photoreceptors. Additionally, DFP treatment significantly diminished *Hmox* upregulation within the NSR and RPE following $NaIO_3$-induced oxidative damage (Figs. 3C, 4C). This result suggests that DFP might protect the retina by decreasing oxidative stress.

DFP diminished C3 upregulation in both the neural retina and RPE in the $NaIO_3$ model. This is of interest given that the complement cascade plays an important role in AMD[28] and in experimental models of retinal degeneration, such as light damage.[29] Local production of complement in the retina has been associated with AMD.[30] If DFP can limit local

complement upregulation in the retina in retinal diseases, this may be protective.

Quantification of photoreceptor nuclei in the $NaIO_3$ model is labor-intensive, since undulation of the neural retina precludes use of ONL thickness as an approximation of photoreceptor number. To facilitate photoreceptor quantification for this and future studies, we developed a function of MATLAB to perform this task in a semiautomated fashion. Although our goal was to generate an automatic counting procedure, the derived software procedure still requires limited assistance from the user. Therefore, improvements of the procedure that would allow full automation is one of the avenues for future work.

To support the biological significance of retinal protection by DFP, we assessed retinal function by electroretinography (ERG). Our preliminary ERG data on C57BL/6J mice treated with NaIO3 alone and cotreated with NaIO3 and DFP showed significant protection of the saturating rod and cone b-wave in the DFP-treated group. No difference was observed in the saturating a-wave (data not shown).

DFP was not retina toxic when given to WT mice for 3 months in our prior study.[16] The dose of DFP used in our prior study and this one was about 3-fold the levels given to humans treated for systemic iron overload. Future studies will examine both dose response and dosing frequency. The apparent lack of retinal toxicity of DFP, combined with the evidence that it can protect the retina against iron overload,[16] $NaIO_3$, the *rd6* mutation, and light damage, suggests that it warrants further investigation for potential treatment of diverse retinal disorders.

Acknowledgments

This work was supported by NIH Grant EY015240, Vision Core Grant NIH P30 EY01583-26, Research to Prevent Blindness, the F.M. Kirby Foundation, the Arnold and Mabel Beckman Initiative for Macular Research, the Paul and Evanina Bell Mackall Foundation Trust, and a gift in memory of Dr. Lee F. Mauger.

Disclosure: **M. Hadziahmetovic**, None; **M. Pajic**, None; **S. Grieco**, None; **Y. Song**, None; **D. Song**, None; **Y. Li**, None; **A. Cwanger**, None; **J. Iacovelli**, None; **S. Chu**, None; **G.-S. Ying**, None; **J. Connelly**, None; **M. Spino**, None; **J.L. Dunaief**, ApoPharma Inc. (F), (P)

References

1. Young RW. The renewal of photoreceptor cell outer segments. *J Cell Biol*. 1967;33:61–72.
2. McBee JK, Palczewski K, Baehr W, Pepperberg DR. Confronting complexity: the interlink of phototransduction and retinoid metabolism in the vertebrate retina. *Prog Retin Eye Res*. 2001;20: 469–529.
3. Gu SM, Thompson DA, Srikumari CR, et al. Mutations in RPE65 cause autosomal recessive childhood-onset severe retinal dystrophy. *Nat Genet*. 1997;17:194–197.
4. Jager RD, Mieler WF, Miller JW. Age-related macular degeneration. *N Engl J Med*. 2008;358: 2606–2617.
5. Zarbin MA. Current concepts in the pathogenesis of age-related macular degeneration. *Arch Ophthalmol*. 2004;122:598–614.
6. Li CM, Chung BH, Presley JB, et al. Lipoprotein-like particles and cholesteryl esters in human Bruch's membrane: initial characterization. *Invest Ophthalmol Vis Sci*. 2005;46:2576–2586.
7. Donoso LA, Kim D, Frost A, Callahan A, Hageman G. The role of inflammation in the pathogenesis of age-related macular degeneration. *Surv Ophthalmol*. 2006;51:137–152.
8. McGeer EG, Klegeris A, McGeer PL. Inflammation, the complement system and the diseases of aging. *Neurobiol Aging*. 2005;26(suppl 1):94–97.
9. Hollyfield JG, Bonilha VL, Rayborn ME, et al. Oxidative damage-induced inflammation initiates age-related macular degeneration. *Nat Med*. 2008;14:194–198.
10. Cai J, Nelson KC, Wu M, Sternberg P Jr, Jones DP. Oxidative damage and protection of the RPE. *Prog Retin Eye Res*. 2000;19:205–221.
11. Age Related Eye Disease Study Research Group. A randomized, placebo-controlled, clinical trial of high-dose supplementation with vitamins C and E, beta carotene, and zinc for age-related macular degeneration and vision loss: AREDS report no. 8. *Arch Ophthalmol*. 2001;119:1417–1436.
12. Kliffen M, van der Schaft TL, Mooy CM, de Jong PT. Morphologic changes in age-related maculopathy. *Microsc Res Tech*. 1997;36:106–122.
13. Hahn P, Milam AH, Dunaief JL. Maculas affected by age-related macular degeneration contain increased chelatable iron in the retinal pigment epithelium and Bruch's membrane. *Arch Ophthalmol*. 2003;121:1099–1105.

14. Hahn P, Qian Y, Dentchev T, et al. Disruption of ceruloplasmin and hephaestin in mice causes retinal iron overload and retinal degeneration with features of age-related macular degeneration. *Proc Natl Acad Sci U S A*. 2004;101:13850–13855.
15. Hadziahmetovic M, Dentchev T, Song Y, et al. Ceruloplasmin/hephaestin knockout mice model morphologic and molecular features of AMD. *Invest Ophthalmol Vis Sci*. 2008;49:2728–2736.
16. Hadziahmetovic M, Song Y, Wolkow N, et al. The oral iron chelator deferiprone protects against iron overload-induced retinal degeneration. *Invest Ophthalmol Vis Sci*. 2011;52:959–968.
17. Li ZL, Lam S, Tso MO. Desferrioxamine ameliorates retinal photic injury in albino rats. *Curr Eye Res*. 1991;10:133–144.
18. Zhu Y, Zhang L, Gidday JM. Deferroxamine preconditioning promotes long-lasting retinal ischemic tolerance. *J Ocul Pharmacol Ther*. 2008;24:527–535.
19. Hidajat RR, McLay JL, Goode DH, Spearing RL. EOG as a monitor of desferrioxamine retinal toxicity. *Doc Ophthalmol*. 2004;109:273–278.
20. Kameya S, Hawes NL, Chang B, Heckenlively JR, Naggert JK, Nishina PM. Mfrp, a gene encoding a frizzled related protein, is mutated in the mouse retinal degeneration 6. *Hum Mol Genet*. 2002;11:1879–1886.
21. Hawes NL, Chang B, Hageman GS, et al. Retinal degeneration 6 (rd6): a new mouse model for human retinitis punctata albescens. *Invest Ophthalmol Vis Sci*. 2000;41:3149–3157.
22. Bergen T, Steckhan D, Wittenberg T, Zerfass T. Segmentation of leukocytes and erythrocytes in blood smear images. *Conf Proc IEEE Eng Med Biol Soc*. 2008;2008:3075–3078.
23. Franco LM, Zulliger R, Wolf-Schnurrbusch UE, et al. Decreased visual function after patchy loss of retinal pigment epithelium induced by low-dose sodium iodate. *Invest Ophthalmol Vis Sci*. 2009;50:4004–4010.
24. Obolensky A, Berenshtein E, Lederman M, et al. Zinc-desferrioxamine attenuates retinal degeneration in the rd10 mouse model of retinitis pigmentosa. *Free Radic Biol Med*. 2011;51:1482–1491.
25. Boddaert N, Le Quan Sang KH, Rotig A, et al. Selective iron chelation in Friedreich ataxia: biologic and clinical implications. *Blood*. 2007;110:401–408.
26. Song D, Song Y, Hadziahmetovic M, Zhong Y, Dunaief JL. Systemic administration of the iron chelator deferiprone protects against light-induced photoreceptor degeneration in the mouse retina. *Free Radic Biol Med*. 2012;53(1):64–71.
27. Rouault TA, Tang CK, Kaptain S, et al. Cloning of the cDNA encoding an RNA regulatory protein–the human iron-responsive element-binding protein. *Proc Natl Acad Sci U S A*. 1990;87:7958–7962.
28. Gehrs KM, Jackson JR, Brown EN, Allikmets R, Hageman GS. Complement, age-related macular degeneration and a vision of the future. *Arch Ophthalmol*. 2010;128:349–358.
29. Rohrer B, Guo Y, Kunchithapautham K, Gilkeson GS. Eliminating complement factor D reduces photoreceptor susceptibility to light-induced damage. *Invest Ophthalmol Vis Sci*. 2007;48:5282–5289.
30. Newman AM, Gallo NB, Hancox LS, et al. Systems-level analysis of age-related macular degeneration reveals global biomarkers and phenotype-specific functional networks. *Genome Med*. 2012;4:16.